Aerodynamic Coefficients Increment due to Plane Flap at Low Reynolds number

Nea Ylilammi, nea_ylilammi@blue1.fi
Helsinki University of Technology - TKK, Otakaari 1, FI-02150 Espoo, Finland

André Valdetaro Gomes Cavalieri, andre@ita.br
Roberto da Mota Girardi, girardi@ita.br
Tiago Barbosa de Araújo, araujotb@ita.br
Instituto Tecnológico de Aeronáutica, Praça Mal. do ar Eduardo Gomes, 50, Vila das Acácias - São José dos Campos - SP - Brazil

Abstract. *In the past few years the interesting on aerodynamics flow over airfoils, with and without flaps, at low Reynolds number has grown substantially. This is due to its applications on micro and unmanned aerial vehicles, which has smaller dimensions than a conventional airplane leading to a smaller Reynolds number of flight. The Technological Institute of Aeronautics (ITA) has studied low Reynolds number flow aiming the manufacturing of unmanned aerial vehicles (UAV). During the first UAV manufacturing a great number of data was generated, which now can be used to the prediction of aerodynamic characteristics for new aircrafts. Among this data there are tests with airfoils fitted with plane flap. Due to the flap there are increments on the main aerodynamic coefficients, such as lift, drag and pitch moment. In this article we show experimental data for some these increments comparing then with semi-empirical methodology used to conventional airplane. Observing that it fits to flap increments predictions and control derivatives for UAV.*

Keywords: *Aerodynamic coefficients, Plane flap, Low Reynolds number*

1. Introduction

During the past three decades the interest in design and development of unmanned aerial vehicles (UAVs) has increased due to their suitability for many varieties of mission types. Especially remotely or autonomously piloted UAVs are ideal to work in hard, repetitive and dangerous tasks that contain a high pay-to-skill ratio as described by Newcome (2004). Therefore todaySs UAVs have been used in missions related to surveillance, ship decoys, communication relay links as well as detection of electrical, chemical, nuclear and biological materials. These mission types require the UAVs to fly at low altitudes as well as low velocities with long endurance. One major challenge is also the durability of air gusts and other weather conditions since the masses of UAVs are wished to be as low as possible. Mueller and DeLaurier (2003) listed the general properties of small UAVs, and according to their publication the UAVs are required to fly at altitudes between 3 to 300 meters with flight duration of 20 to $100km/h$. The masses of these vehicles are less than $25kg$ with a wing spans lower than 6 meters.

Due to these requirements the UAVs are set to fly inside a low chord Reynolds number (Re) range. Because of the technological developments in data collection techniques in the form of smaller video cameras and sensors as well as control hardware the Reynolds numbers are getting even lower into a more critical flow velocity range as flown by micro-air vehicles (MAVs), the masses and wing spans of which can be as low as $80g$ and $15cm$. For these Reynolds numbers ranging from approximately 1.5×10^4 to 5.0×10^5, a number of differences occur in the flow properties when compared to those for higher Reynolds numbers. These are the presence of hysteresis in the aerodynamic curves, laminar separation bubble, non-linearity in the lift curve slope and the position of transition from laminar to turbulent flow as discussed by Carmichael (1981), Selig et al (1996) and Mueller and DeLaurier (2003). Although a number of studies have been published about the problems related to this flow velocity range and multiple airfoils have been developed for existing and future UAVs, not much aerodynamic data exists for wing sections with high-lift devices. Therefore more studies are required in order to develop more accurate and efficient design techniques for safe and reliable UAVs, as pointed out by Girardi et al. (2007).

In the current work the aerodynamic parameters of a $NACA$ 2412 airfoil with a plain flap of 30% chord length were measured with 13 different flap deflections ranging from -30 to 30 degrees by every 5 degrees. The tests were ran with 6 different Reynolds numbers varying from 3.9×10^4 to 2.6×10^5 in order to achieve a good overall knowledge of the flow properties over the tested airfoil in a critical Reynolds number range typical for future small UAVs. The results were then compared to the values given by existing calculation methods developed by Roskam (2000) that is used in the aerodynamic design of wing sections of higher Reynolds numbers. The applicability of these methods was then studied and some calculation techniques were developed in order to correct the inaccuracies found. The achieved results can be used as a starting point in the design of wing with an aileron or a horizontal tail with an elevator.

2. Experimental Apparatus

The measurements were performed in ITA's open jet wind tunnel which has a squared test section as shown in Figure 1 (a) below. The test section has geometric measures of $460mm$ and its corners have been filled with triangular fillets whose dimension change along the wind tunnel length. This eliminates the boundary layer growth along the test section and hence maintains a constant static pressure. The flow velocity range of the tunnel varies from 4 to $30m/s$ and the turbulence intensity at the highest velocity is 0.5%.

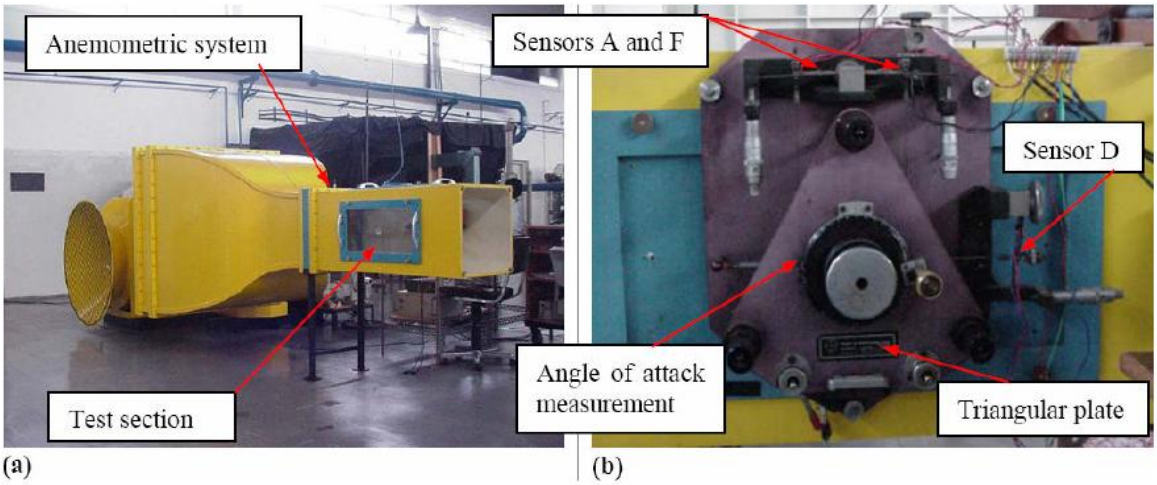

Figure 1. Open jet wind tunnel with square test section characterized by the dimension of $460mm$ (a) and the aerodynamic balance used for force measurement (b).

The force measurements were performed with a triangular balance plate shown in Figure 1 (b). This balance was fixed to the lateral wall outside the tunnel. The used model was attached to the balance with a metal axis fixed in the model, which also transmitted the aerodynamic forces to the balance. Lift, drag and pitching moment were measured with the balanceŠs three load cells that were connected to the wind tunnel structure. These load cells were actually metal plates instrumented with four strain gages that formed a complete Wheatstone bridge. As indicated in Figure 1 (b) these load cells are called here as sensors A, F and D. Sensors A and F were used to measure the lift and pitching moment and sensor D measured the experienced drag.

Each load cell was connected to an amplifier and a filter that functioned as an independent signal conditioner module allowing proper adjustment of the output voltage before the connection to the computer based data acquisition system. In this experiment the maximum output voltage of each sensor was chosen to be 10 volts to maximize the measurement resolution. The anemometric system, located at the contraction' end, uses a Pitot tube for dynamic pressure measurements. This Pitot tube is connected to a pressure transducer, which is also wired to a signal conditioner and to the acquisition system. From figure 1 we can see the device used for changing the angle of attack, which is done manually.

The model tested in this is a NACA 2412 equipped with a 30% chord plain flap, as shown in figure 2. The metal hinge used to connect the plain flap to main airfoil causes a $2mm$ gap. The metal axis (see figure 2) used to connect the model to the experimental apparatus located 38.1 mm from the leading edge which is at the quarter-chord of the airfoil. The figure 2 also shows the airfoil dimensions and the device used for keep the flap angle fixed, item (c), varying it for each 5 degrees.

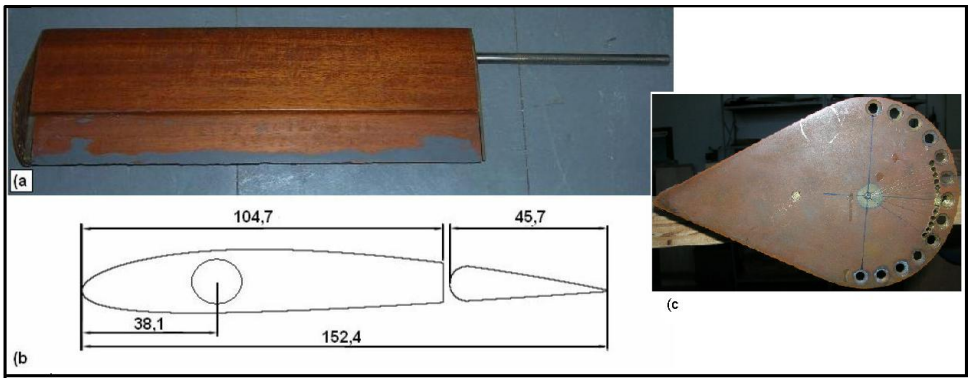

Figure 2. Model NACA 2412 used into the experiments (a) and schematic sketch with its dimensions (b) in millimeters.

3. Experimental Procedure

As shown in the previous section the force measurements is done using the aerodynamic balance, that consist in three load cells equipped with strain gages, which gives a linear electrical response to applied force. This load cells are calibrated using a system of pulleys and standard masses, as shown in figure 3, where the wires links a metal axes, which transmits the force applied to the balance by the standard masses in a plate fixed at the wire end. The configuration presented in the figure 3 (a) is used to calibrate the sensor D, used for drag measurements, while the configuration shown in the item (b) is used for calibrating the sensors A and F used for measuring the lift and pitching moment.

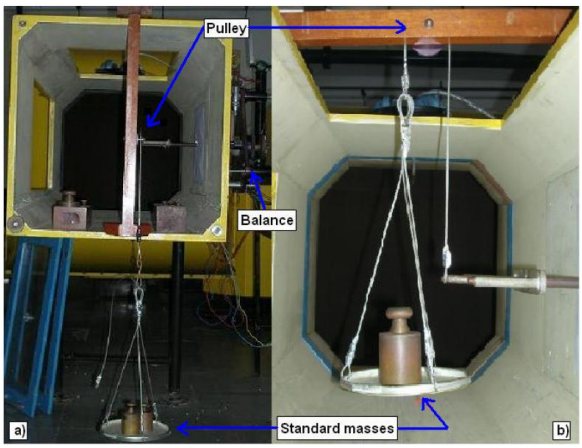

Figure 3. Calibration system for the sensor D (a) and A and F (b).

The calibration was done by incrementing loads from zero to the maximum value estimated for the load cell in question and then down to zero again. Approximately 20 different loads were used in every calibration process and during a sampling time of one second, 1000 measurements were performed. The average value of these measurements was then correlated with the imposed force. A similar kind of methodology is applied for pressure transducer calibration, using a Betz manometer as standard ranging from 0 to 100 mmH_2O.

With the calibration done, Then alignment of the airfoil was performed with the help of an attached drawing at the test section wall. The inaccuracy in the alignment was approximated to be $\pm 1mm$ which equals to uncertainty of ± 0.5 degrees in the angle of attack. After the alignment, the initial signals of the four sensors were read by the acquisition system. This was done with the same vibration used at the calibration process in order to insure that all the load cells were well accommodated.

After measuring the initial voltages while keeping the flow velocity zero, the wind tunnel was turned on and the wanted dynamic pressure was adjusted. This flow velocity is then kept constant during all the measurements with different flap angles. The measurements for each flap angle were then performed with different angles of attack, starting from negative value by increments of two degrees for the linear part of the curve and increments of one degree near de stall. The presence of a laminar separation bubble was then tested by decrementing the angle of attack below the stall angle and observing the possible hysteresis behavior.

During the measurements a data acquisition code written in the LabView ambient performed the measurements of the aerodynamic forces experienced with the balanceŠs three load cells and the dynamic pressure experienced with the pressure transducer. For every measuring point all the four signals were sampled 5000 times during a sampling time of 5 seconds and with a sampling rate of 1000 Hz. The using the calibration coefficients the mean values from these measurements are used for the reduction, which give us the actual forces and pressure values.

The procedure presented in the previous is repeated for the six Reynolds number (Re) presented in this paper. However for the two lowest Re, 3.9×10^4 and 6.1×10^4, the values has occurred some problem with the lift results for different flap angles. The results for $Re = 6.1 \times 10^4$, for example could be observed that the lift for flap angle of 15 degrees gave the highest values instead of the lift curve achieved with the flap angle of 30 degrees, behaving different from the expected. The most probable cause for this being erratic initial values measured with the wind tunnel off, which was confirmed by a set of checking experiments. So, this problem was solved by using mean initial values, eliminating the erratic measurements, for all the load cells.

4. Results

This section is devoted to present the results obtained for the Reynolds and flap angle variations. The results consist in lift and pithing moment for six Reynolds number and thirteen angles of attack, however, due to the paper limitations we are just going to present the figures containing the variations due to flap deflections. The uncertainty for the lift and

moment measurements was estimated by the methods given by AIAA (1999) to be 6%, for the drag the same was 2% and finally 3% for the dynamic pressure values. This is not going to bee shown in the graphics for better understanding.

In the figure 4 is presented the variation of the lift slope curve as a function of the Reynolds number, for zero angle flap deflection. Is also presented the results obtained by Prudente (2005) for the same model and the Roskam (2000) present theory, which is applied to higher Re. All the results for the lift coefficient were corrected with the procedure described by Gomes (2005) in order to eliminate the blockage effect.

Nonlinearities at the lift curve slopes are present especially for the higher flap deflections as the flow velocity is lowered which in turn decreases the effective camber of the airfoil. The boundary layer thickness increase is caused by an observed separation bubble.

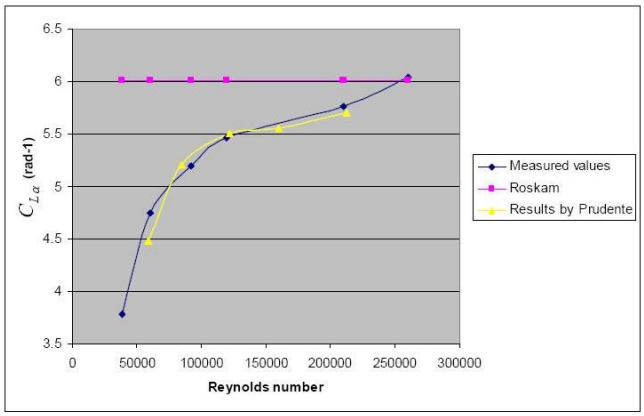

Figure 4. Lift curve slope variation with Reynolds number for zero flap deflection.

As it can be observed from the results, there is a decrease in the lift curve slopes as the Reynolds number is lowered, caused by the decreases in effective airfoil camber. As already pointed out by Schlichting and Truckenbrodt (1979), this viscosity effect increases as the angle of attack is deflected and hence the lift curve slope for these Reynolds numbers becomes lower.

Based to the measured results a corrective calculation term was developed in order to correct the inaccuracy in comparison to the calculated values. This was done simply by taking a second order polynomial curve from the measured results that was then reduced from the results given by Roskam (2000). According to this procedure the lift curves for the tested airfoil can be calculated by reducing the following term given in equation 1 from the results first calculated by the existing Roskam‘s method used for the higher Reynolds numbers as is shown by equation 2.

$$\Delta C_{L\alpha} = -6 \times 10^{-16} Re^3 + 3.25 \times 10^{-10} - 5.985 \times 10^{-5} + 4.0677 \tag{1}$$

$$C_{L\alpha} = C_{L\alpha - Roskam} - \Delta C_{L\alpha} \tag{2}$$

Where $C_{L\alpha - Roskam}$ is the lift curve slope calculated by Roskam‘s methodology and $\Delta C_{L\alpha}$ is the corrective constant for Reynolds number effect, presented in the figure 5.

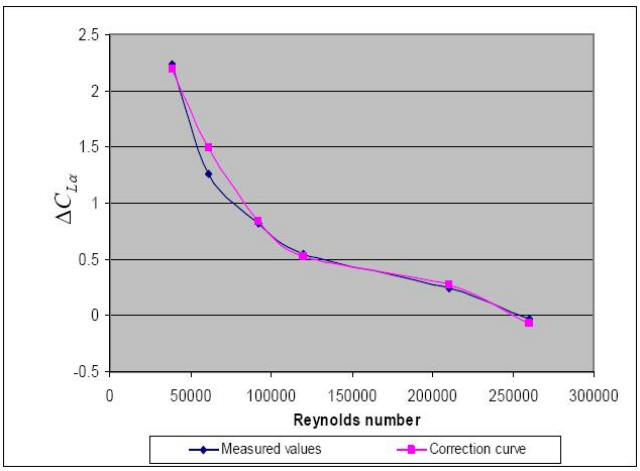

Figure 5. Lift curve slope correction for different Reynolds number.

In Figure 6 the lift increment at zero angle of attack for the tested Reynolds numbers are presented as a function of the flap angle. Also the results given by Roskam (2000) are plotted here in order to compare these results. The used calculation method does not provide information for the negative flap deflections and hence this comparison could not be performed for these parts of the measured curves. As it can be observed, the experimental results are lower than the ones given by the calculation technique used for higher Reynolds numbers. Hence this method should not be used in the flow regime in question and a corrective calculation procedure needs to be developed for this flow velocity range that also includes the effect of the Reynolds number.

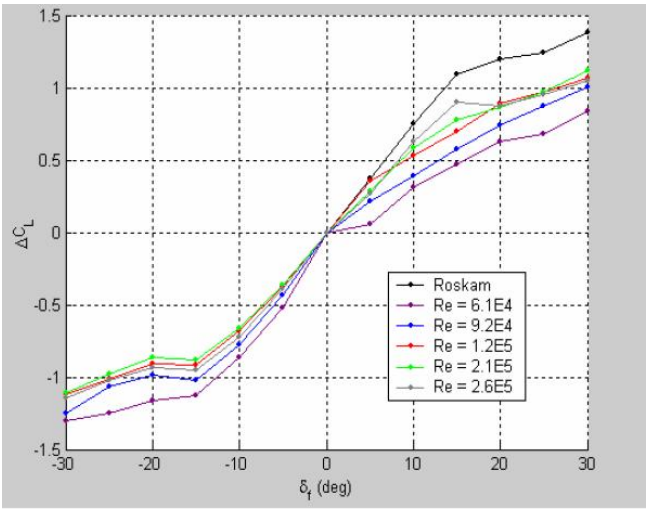

Figure 6. Lift increments for different flap deflections at zero angle of attack.

In order to develop a precise calculation method that could be used for reliable predictive design of all kinds of wing sections, a large amount of airfoil data needed to be collected and combined. However, with the results gathered from the performed measurements in this work, corrective curves were created that can be used as a directional guidance in the preliminary design process of UAVs‘ wing sections with ailerons or tail sections with elevators.These corrective curves are presented in Figure 7, from which the effect of the Reynolds number for different flap deflections can be corrected by multiplying the read correction factor $k_{Re}(\Delta C_L)$ with the lift increment calculated from the method given by Roskam (2000). For clearance, this is also presented as an equation 3:

$$\Delta C_L = k_{Re}(\Delta C_L)\Delta C_{L-Roskam} \tag{3}$$

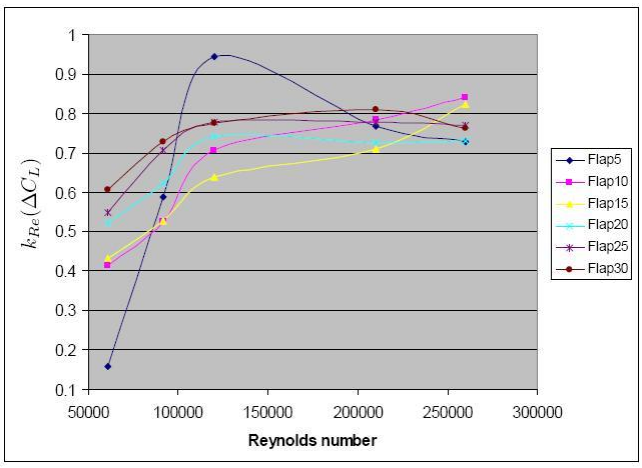

Figure 7. Lift increment correction curves for different flap deflections as a function of Reynolds numbers.

In Figure 8 the increment in the maximum lift coefficient is presented for each Reynolds number measured as a function of the flap deflection. Also as before the results calculated with the method given by Roskam (2000) are plotted here in order to make a comparison with the measured values. Although little variation at the maximum values of the lift coefficient can be observed for the Reynolds number of 6.1×10^4, the effect of the lower flow velocity can be seen

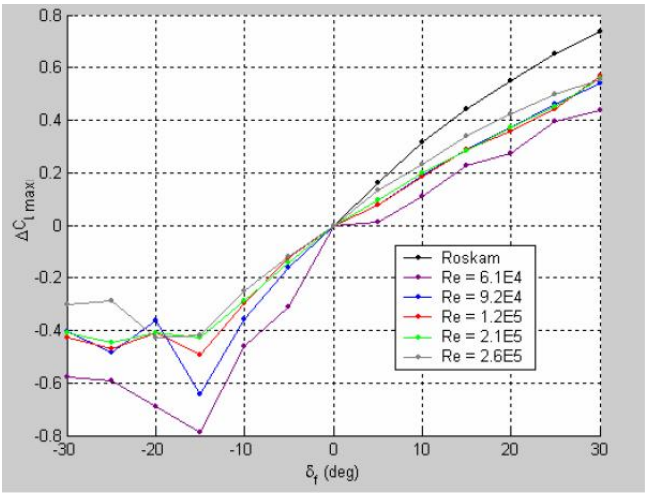

Figure 8. Maximum lift increments for different flap deflections at zero angle of attack.

here as a reduction on the maximum values. It can be noticed that the presented calculation method is not accurate for the Reynolds number regime studied and a corrective prediction method needs to be developed for the design of UAVs.

As for the lift increment, a similar kind of corrective curves were created from the measured values collected for NACA 2412 and these results are presented in Figure 9. Again a corrective calculation can be performed for the airfoil in question by multiplying the correctional constant $k_{Re}(\Delta C_{Lmax})$ with the results estimated with the information provided by Roskam (2000). In a form of equation:

$$\Delta C_{Lmax} = k_{Re}(\Delta C_{Lmax})\Delta C_{Lmax-Roskam} \tag{4}$$

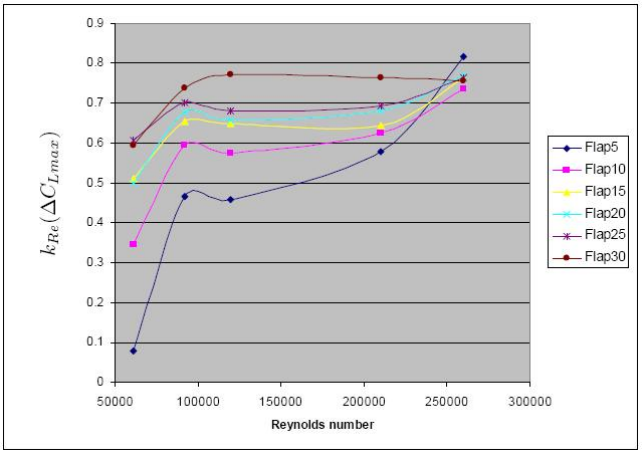

Figure 9. Maximum lift increment correction curves for different flap deflections as a function of Reynolds numbers.

Finalizing, a similar kind of analysis was also done for the pitching moment increment at the zero angle of attack, the results of which are presented in Figure 10. Again the calculated values given by Roskam (2000) are plotted with the measured results in order to make a comparison. As a conclusion the theoretical curve seems to have more negative values than are the ones collected experimentally and hence a corrective procedure should be developed in order to disregard this inaccuracy for the flow regime of interest. Although there seems to be some overlapping and significant variation with the measured moment coefficients, an equivalent correction technique was performed also for the moment increments for different Reynolds numbers as was done for the lift increment. Corresponding corrective curves can be seen from Figure 11 and the use of the corrective coefficient is done as before for the lift increment. Hence the effect of the Reynolds number to the moment increments can be accounted for by multiplying the correction constant $k_{Re}(\Delta C_M)$ with the moment increment achieved with the help of Roskam‘s technique:

$$\Delta C_M = k_{Re}(\Delta C_M)\Delta C_{M-Roskam} \tag{5}$$

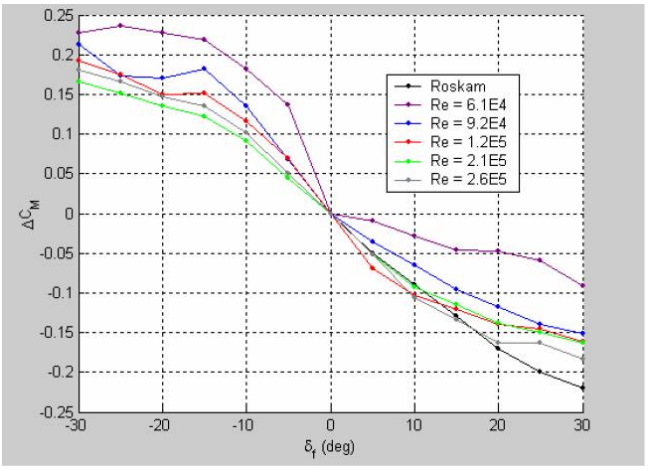

Figure 10. Moment increments for different flap deflections at zero angle of attack.

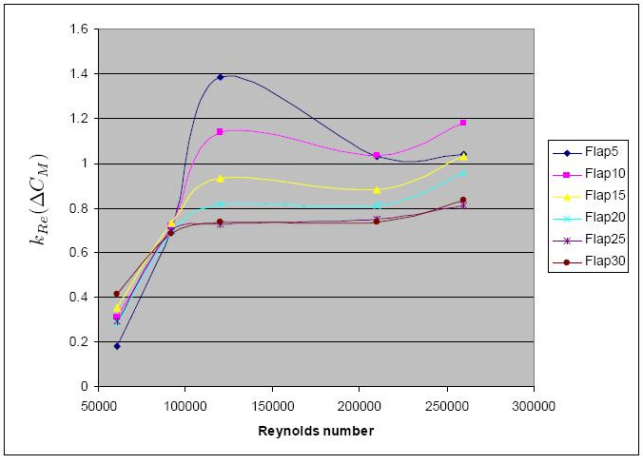

Figure 11. Moment increment correction curves for different flap deflections as a function of Reynolds numbers.

5. Final Remarks

The measurements performed in the current work showed the problematic nature of experimental studies in the low Reynolds number regime typical for unmanned aerial vehicles. It was noted that the measuring equipment used, as well as the experimental procedure, needs very good accuracy and all the possible variation should be neglected. Although some corrective methods were presented in order to fix the measured values, these should not be needed and the used experimental apparatus should be improved for future studies in this field.

The collected results showed clearly the differences in the aerodynamic properties when the flow velocities are decreased from the ones typical for manned aviation. As the boundary layers of the airfoils in this Reynolds number regime are laminar, many are the effects caused to the aerodynamic efficiencies of the wing sections. In order to avoid these losses, better prediction methods are needed for the preliminary design for these flow velocities. As could be observed from the collected results for the tested airfoil, the coefficients given by Roskam's (2005) calculation methods accurate for higher Reynolds numbers differ from the actual properties of the wing sections at the flow regime of interest. Hence these prediction estimations techniques need to be corrected for the Reynolds number effect.

Although difficulties were confronted and all inaccuracies in the measured values could not be corrected, corrective methods were created that can be used as guidance in the preliminary design process of UAVs.

6. Acknowledgements

To the Financiadora de Estudos e Projetos (FINEP), for supporting part of the resources used to the Unmanned Aircraft Vehicle development and to the Centro de Estudos de Sistemas Avançados do Recife (CESAR), to the partnership in this project. To the staff of the Prof. K.L. Feng Aeronautical Engineering Laboratory.

7. References

American Institute of Aeronautics and Astronautics, 1999, "Assessment of Experimental Uncertainty with Application to Wind Tunnel Testing A Standard",AIAA S-017A, Washington DC.

Abbott, I. H., 1949, "Theory of Wind Sections: Including a Summary of Airfoil Data", McGraw-Hill, New York.

Carmichael B.H., 1981, "Low Reynolds number airfoil survey", Vol. 1, NASA CR 165803.

Girardi, R.M., Cavalieri, A.V.G. and Araújo, T.B.,2007, "Experimental Determination of the Wing Airfoil Aerodynamic Characteristics and Flap Hinge Moment of the Wing Airfoil used at ITAŠs Unmanned Aerial Vehicle (UAV)", Proceedings of the 19th International Congress of Mechanical Engineering, Brasília, Nov. 5-9.

Gomes, C.D.A.N., 2005, "Avaliação da Razão de Bloqueio Bi-Dimensional Utilizando Método dos Painéis", Trabalho de Conclusão de Curso (Graduação) Ű Instituto Tecnológico de Aeronáutica, São José dos Campos.

Mueller, T. J., DeLaurier, J. D.,2003, "Aerodynamics of Small Vehicles", Annual Review of Fluid Mechanics.

Newcome, L.R., 2004, "Unmanned aviation: a brief history of unmanned aerial vehicles".

Prudente, D. M., 2005, "Theoretical and Experimental Study of Airfoils at Low Reynolds Numbers", Graduation work (in Portuguese), ITA, Sao Jose dos Campos.

Raymer, D. P., 1999, "Aircraft Design: a Conceptual Approach", 3rd edition, AIAA Educational Series, Washington DC.

Roskam, J.,2000, "Airplane Design Part VI: Preliminary Calculation of Aerodynamic, Thrust and Power Characteristics", DARcorporation.

Schlichting, H., Truckenbrodt, E., 1979, "Aerodynamics of the Airplane", McGraw-Hill.

Selig, M.S., Guglielmo, J.J., Broeren, A.P. and Giguere, P., 1996, "Experiments on airfoils at low Reynolds numbers", AIAA, Aerospace Sciences Meeting and Exhibit, Reno, NV, Jan.15-18.

8. Responsibility notice

The author(s) is (are) the only responsible for the printed material included in this paper